

Growth Monitoring of Healthy and BSR-infected Oil Palm Seedlings Using Ground-based LiDAR

Nur Azuan Husin^{1,2*}, Ray Clement Ridu², Normahnani Md Noh³ and Siti Khairunniza Bejo^{1,2,4}

¹Smart Farming Technology Research Centre, Universiti Putra Malaysia, 43400 UPM, Serdang, Selangor, Malaysia

²Department of Biological and Agricultural Engineering, Faculty of Engineering, Universiti Putra Malaysia 43400 UPM, Serdang, Selangor, Malaysia

³Sime Darby Plantation R&D Centre, KM 10, Jalan Banting-Kelanang, 42700, Banting, Selangor, Malaysia

⁴Institute of Plantation Studies, Universiti Putra Malaysia, 43400 UPM, Serdang, Selangor, Malaysia

ABSTRACT

The most threatening disease to the oil palm is Basal Stem Rot (BSR) disease caused by *Ganoderma boninense*. Besides matured oil palm trees, palm seedlings are susceptible to BSR disease. Therefore, it is crucial to detect the symptoms of the disease at an early stage so that the infected plants can be treated immediately. This study focuses on growth monitoring to differentiate between the infected (INF) seedlings and non-infected (NONF) seedlings by using ground-based LiDAR. This study used one hundred INF seedlings and 20 NONF seedlings, where the NONF seedlings acted as a control. The parameters measured using LiDAR were the height, stem diameter, and point density of the seedlings, which were measured four times every two-week intervals. The results showed significant differences in mean height and mean stem diameter between INF and NONF seedlings. Results from the LiDAR measurements were consistent with the manual measurements, with more than 86% correlations. In temporal measurements, the mean stem diameter for NONF seedlings consistently increased over the six weeks, while for INF seedlings, it was inconsistent throughout the time. Furthermore, in the last three measurements, the mean point density of NONF seedlings was higher than that of INF seedlings, which indicated better growth of non-infected seedlings than infected seedlings.

ARTICLE INFO

Article history:

Received: 29 May 2024

Accepted: 04 November 2024

Published: 26 March 2025

DOI: <https://doi.org/10.47836/pjst.33.3.03>

E-mail addresses:

nurazuan@upm.edu.my (Nur Azuan Husin)

rayclement98@gmail.com (Ray Clement Ridu)

normahnani.md.noh@simedarby-plantation.com (Normahnani Md Noh)

skbejo@upm.edu.my (Siti Khairunniza Bejo)

* Corresponding author

Keywords: *Ganoderma boninense*, height, infected oil palms, point clouds, stem diameter

INTRODUCTION

Elaeis guineensis, or oil palm, is widely planted throughout Southeast Asia, where Malaysia is the world's second-largest producer of palm oil. The planted area

reached 5.67 million hectares in 2022, with most of the area in Sabah and Sarawak encompassing 3.13 hectares (Parveez et al., 2022). Over the last 30 years, the annual exports have been increasing steadily, thus making palm oil and palm-based products among the top 10 exports in the country. Oil palm is the most beneficial vegetable oil plant, which can be harvested for more than 25 years (Yap et al., 2021). In other oil-producing crops such as soybean and rapeseed, the output-to-input energy is 3:1, whereas the oil palm output-to-input energy ratio is higher, 9:1 (Farraji et al., 2021).

The most threatening disease to the oil palm is the Basal Stem Rot (BSR) disease caused by *Ganoderma boninense* (*G. boninense*). The disease could cause a reduction of fresh fruit bunch (FFB) yield up to 4.3 tonnes per hectare (Husin et al., 2020a). An estimated RM2.2 billion in economic losses are incurred annually by Malaysia due to the fact that diseased trees are present in approximately 60% of plantation areas (Bharudin et al., 2022). Over the last 30 years, the annual exports have been increasing steadily, thus making palm oil and palm-based products among the top 10 exports in the country. The disease can affect mature trees and oil palm seedlings, with the latter group experiencing earlier and more severe symptoms (Azmi et al., 2020). The symptoms of a *G. boninense* infection resemble those of water stress and nutrient deprivation because *G. boninense* generates enzymes that have the potential to break down cellulose, lignin layers, woody tissues, and xylem, significantly disrupting the flow of nutrients and water to the upper portion of the palm. There are no notable symptoms that the unaided eye may observe, so it is challenging to identify BSR signs in its early phases (Khairunniza-Bejo et al., 2021).

When oil palm seedlings are infected with *G. boninense*, the first noticeable symptom is the appearance of fruiting bodies at the bole part. The fronds then exhibit mottling or partial leaf yellowing, and when more than 50% of the stem base has been internally destroyed, necrosis occurs. However, the fruiting body may or may not appear prior to the development of foliar symptoms, making visual identification difficult and commonly overlooked. In severe situations, the incapacity to complete photosynthesis may result in reduced development, particularly in girth, height and frond count (Zevgolis et al., 2022). However, because a fungal mass can emerge before or after leaf withering, it can be difficult to see with the unaided eye and frequently goes unnoticed. Infection with *G. boninense* can also be found in the longitudinal sectioning and roots of the infected bole, even in the absence of visible symptoms (Azmi et al., 2021). A dark discolouration and white mycelium poking through the root epidermis are typically seen in the longitudinal section, which indicates an upward infection progression within the seedling. However, because it is a labour-intensive procedure that can destroy trees, bole and root detection is not practicable in large-scale plantations. In typical nursery practice, a human-performed manual census is utilised to track the course of the disease in relation to different treatments. A human examination mostly depends on the disease's outward manifestations. This approach is prone to inaccuracy because of little experience, arbitrary assessments, and situations with no symptoms.

Some researchers have used laboratory methods for *Ganoderma* BSR disease detection. Madihah et al. (2014) developed immunoassay-based detection methods for *G. boninense* detection using Enzyme-linked immunosorbent assay (ELISA), which uses both monoclonal and polyclonal antibodies. Meanwhile, Akul et al. (2018) used Loop-mediated isothermal amplification (LAMP), which consists of two outer and two inner primer sets of the target DNA, to specifically identify the manganese superoxide gene (MnSOD) of *G. boninense* for the BSR disease detection in oil palm. Madihah et al. (2018) also used the LAMP method, where only the bug1A primer combination, out of eight sets of LAMP primers, which could differentiate between other actinomycetes/basidiomycetes fungus and *Ganoderma* non-pathogenic strains and pathogenic strains (*G. boninense*). In addition, Hilmi et al. (2022) used the Polymerase chain reaction (PCR) method created using a primer based on the ribosomal DNA internal transcribed spacer (ITS) region to identify a pathogenic *Ganoderma* species. The laboratory-based methods are reliable for early detection of the disease, but the cost is high, the procedure is complex and time-consuming, and some are unsuitable for outdoor conditions (Azuan et al., 2019).

Remote sensing technology is a method that is reliable, fast, and suitable for outdoor activity. Laser scanning or LiDAR (Light Detection and Ranging) is one of the popular remote sensing techniques. A laser scanner uses high-speed laser technology to acquire millions of laser points to generate a three-dimensional (3D) set of data in space known as point clouds in a significantly short time. 3D laser scanners have the potential to distinguish information about plant biomass or plant architecture. Single plant organs can be determined automatically, and the volume of information can be determined, which has been shown to have a high correlation to the actual measurement (Buja et al., 2021). The benefits of LiDAR-based systems over passive ones - which are limited by variations in light, atmospheric conditions, viewing angle, and canopy structure - include enhanced data-gathering flexibility, a high degree of automation, and the ability to deliver data at a rapid pace. The application of machine learning techniques for spatially and temporally distributed big data, along with a multi-sensor systems approach that focuses on conventional optimal estimation, can lead to increased accuracy in plant disease detection (Husin et al., 2022). One such technique is the fusion of LiDAR with existing electro-optical sensors. These electro-optical sensors provide novel ways to predict and respond to plant disease when used on a range of platforms, including satellites, ground-based robotic vehicles, handheld devices, and aerial vehicles. LiDAR technology can be used in oil palm fields due to the benefits of obtaining detailed three-dimensional (3D) data without physical contact with the scanned object.

Crop health monitoring is increasingly using remote sensors, which provide plant disease detection and quantification at many evaluation levels in a non-destructive, spatialised manner. The advancement of sensor technology has helped the development of new precision agricultural techniques. Emerging methodologies for acquiring phenotypic

features through LIDAR shape profiling have been established, with the major metrics being the height and leaf area density (Fahey et al., 2020). Similarly, as part of a high-throughput characterisation platform, LIDAR shape profiling is used to assess the canopy and above-ground biomass. The information could be used to analyse physiological growth and detect different substances in plants for ecological applications such as disease detection. The analysis of the use of LiDAR in phenotyping is still in its infancy, but the depth and variety of information provided by LIDAR in a short amount of time at a low cost, particularly in relation to plant structure, is advantageous. Metric measurements of trees were obtained using the laser scanning method, where various tree characteristics were extracted, i.e., diameters at breast height and tree height (Cabo et al., 2018; Liu et al., 2018), crown diameter, crown area, height and tree volume (Wagers et al., 2021), crown base height, crown diameter and crown volume (Hillman et al., 2021) and diameter, stem curve and height measurements, crown width (Pitkänen et al., 2021) with high correlations and accuracies. Therefore, the applications of laser scanners for metric measurements were proven for accurate metric measurements aimed at growth monitoring and could be used for disease detection. For example, a Terrestrial Laser Scanner (TLS) was used by several researchers (Azuan et al., 2019; Husin et al., 2020a) to study the physical characteristics of mature oil palm trees on a plantation. Several parameters such as crown size, oil palm frond's number, the gap between the oil palm fronds (measured in degree), number of unopened new fronds (also known as spears), perimeter and area of the trunk were used to detect and determine the level of BSR disease infection (Husin et al., 2020b; Husin et al., 2020c). These parameters were measured in different levels of infections, thus using statistical analysis, detection models, and machine learning integration. Early detection of BSR disease was done, and infected and non-infected oil palm trees were discriminated successfully.

Temporal data on palm seedling oil is important for monitoring the conditions of the seedlings and for offering disease-related data that can help clarify the course and dissemination of the disease (Husin et al., 2022). Meanwhile, the compilation and analysis of temporal data can be used to diagnose the disease early in advance of a potential diagnostic outbreak (Santoso et al., 2011; Azahar et al., 2011). Therefore, the objectives of this study were to measure the changes in oil palm seedlings due to infection of BSR disease using temporal data and to differentiate between healthy and BSR-infected oil palm seedlings using point cloud images taken by ground-based LiDAR sensors, also known as Terrestrial Laser Scanner (TLS). It is hypothesised that enzymes produced by *G. boninense* fungus have impaired the xylem and phloem tissues, which are essential for storing and moving water and carbohydrates in plants. Infected seedlings may endure significantly low carbohydrate intakes and severe water deficiencies that restrict the plant's ability to perform regular photosynthesis. These would inhibit tree growth and affect the physiological conditions of the seedlings, such as the diameter of the stem, the plant's height, and total

point density, which can be measured. The study could be used to differentiate between infected and uninfected oil palm seedlings towards an early detection approach and management control of the disease (Husin et al., 2021).

MATERIALS AND METHODS

Study Area

The study was conducted in an oil palm greenhouse nursery located at Sime Darby Plantation Banting, Selangor, Malaysia (2°48'08.6" N, 101°27'33.0" E). The greenhouse was utilised to cultivate all seedlings, maintaining regulated humidity and temperature levels, where the area was 16 m length × 6 m width × 2 m height. The roof and the wall were made from transparent UV plastic, and black netting was used to cover them. UV plastic was used to prevent the seedlings from getting excess water from the rain and harmful UV light, while black netting was used to reduce heat from the sun. There was a control system that could automatically adjust the amount of water and fertilisers applied to all the seedlings; therefore, all the seedlings could be monitored. The temperature of the greenhouse was averaged at 27°C, and the humidity was about 90%. The seedlings used for this study were Tenera hybrids, and the seedlings were eight months old. One hundred BSR-infected seedlings (INF) were inoculated with *G. boninense* inoculum (Naidu et al., 2018) by attaching a colonised *G. boninense* rubberwood block to the roots of the seedlings for five months, and only 20 healthy seedlings (NONF) were used as a control.

The arrangement of seedlings in the greenhouse was as follows: five lines of infected seedlings and one line for non-infected seedlings, each consisting of 20 seedlings at a distance of 0.5 m apart from each other. Six water tanks were placed in the middle of the greenhouse to supply water through a drip irrigation system, where the seedlings received approximately 1.0 L/polybag/day. They were fertilised with 50 g nitrogen (N), phosphorus (P) and potassium (K) solid fertiliser according to plantation practice. Biosafety guidelines were followed by implementing the Integrated Ganoderma Management (IGM) system by all the personnel and researchers working in the nursery facilities. The infected and non-infected plants were placed without barriers according to plantation practices. The infection process that occurs after root contact with an infection source has been proven by years of extensive investigation, both in the lab and the field (Rees et al., 2009). In the early stages of the disease, spores were not involved, while both the infection process and bracket formation on young, infected palms did not contribute to the same (Sanderson, 2005).

For data gathering, the scanner was positioned atop a surveying tripod at a height of approximately one metre. The area was scanned from eight scan points to capture the 3D image of the seedlings (Figure 1). Six high-reflective sphere references were arranged at a specific point that could be detected from all scan points. The function of the sphere

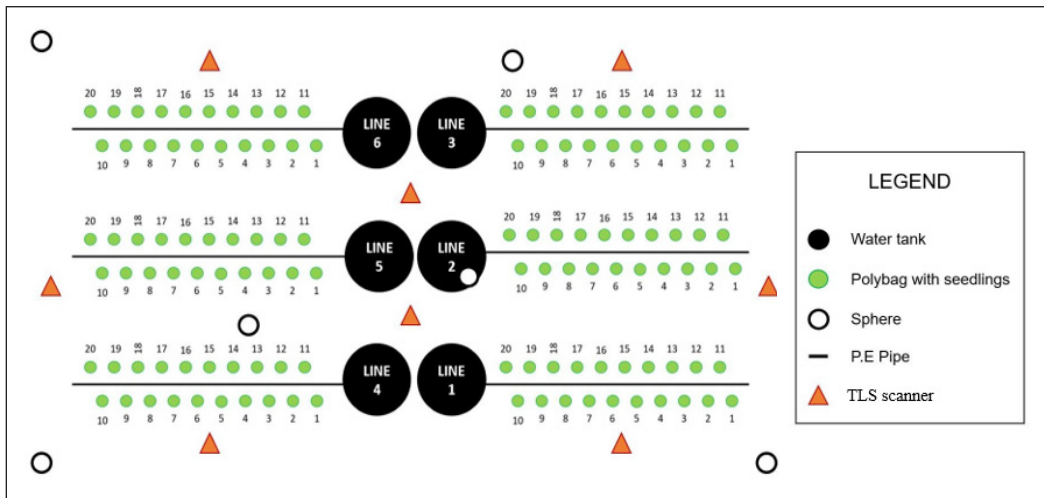


Figure 1. Setup of data acquisition

was to transform the multiple different views of images into the same coordinate frame. Despite the position of the scan, the geometry of the spheres was noticeable, and it was easily used to merge the scan files in case it could not detect the scan locations (Bornaz & Rinaudo, 2004). The data acquisitions were taken every two weeks.

Point Cloud Processing Using SCENE Software

The laser scans were recorded on a removable SD memory card that was subsequently transferred for further analysis using SCENE software (version 6.2, FARO Technologies, Inc.). SCENE is FARO’s processing software for point clouds, where the main steps involved in post-processing are filtering, registration, and extraction of the area of interest (AOI). The “registration” step was completed to match the multiple scan positions and synchronise the laser point data to create a cluster of point clouds. Before filtering, the scan points usually contain noise caused by reflections on water in the polybags and the presence of small particles in the air. Thus, the desired scan points could be corrected, and noise could be removed from the scans by using a filter. The scan point clouds were created first, and then a “clipping box” was used to isolate the AOI from the environment. This enabled “slicing” the point cloud and “clipping” (separate) specific areas as needed to display or hide certain points of the 3D point cloud.

Stem Diameter and Height Measurements

The stem diameter was measured in the SCENE software, where parts of the seedlings were zoomed, and a “measure points” tool was used to obtain the cross-section image of the stem seedlings. The stem diameter was measured at the middle section of the stem,

which was about 2 cm from the base or soil level. Meanwhile, the height of the seedlings was measured from the tip of the plant to the base or soil level and was obtained using CloudCompare software (Cloud Compare [GPL software] v2.9 Omnia). The steps were to save the .pts file from the SCENE point cloud data, import it into the CloudCompare software, and save the file as a .bin file. The format .bin was used because it was smaller and more compatible with the CloudCompare software. Next, the image was converted into a scalar field image in Z coordinates. After that, outliers and unwanted objects, i.e., water tanks and poles, were removed through the segmentation process using a “segment” tool and a “cross-section” tool. The top polybags, which were about 40 cm in height, were set as a reference for the ground level to measure the height of the oil palm seedlings. The height was considered from the top of the soil, where all the seedlings had almost the same planting depth. The oil palm seedlings’ point cloud images that were processed in the CloudCompare software are displayed in Figure 2.

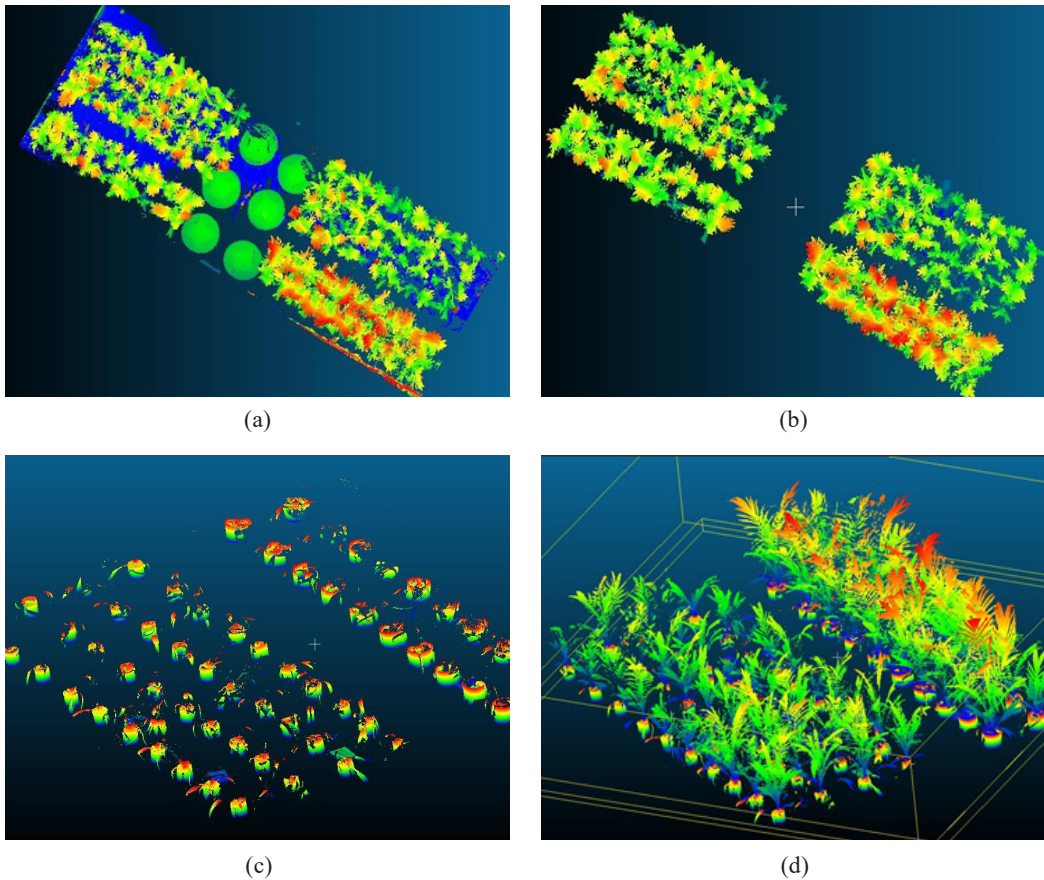


Figure 2. Steps of point cloud processing: (a) Conversion to scalar image; (b) Removal of unwanted objects; (c) Polybags separation; and (d) Metric measurements

Measurements of Point Density

The plant density, which consists of point cloud data, was calculated using the volume density features in the CloudCompare software (Girardeau-Montaut, 2016). LiDAR sensor measured the reflected pulses; therefore, a scanned object with a larger area and volume would reflect higher pulses. A similar approach was used, where a segmentation process was undertaken to remove all the outliers and unnecessary captured objects such as polybags, poles, pipelines and water tanks. After that, the geometric features tool was selected, and then the volume density was ticked to obtain the point density of the NONF and INF oil palm seedlings. The tool's main function was to estimate the volume density captured by TLS by counting each point in the point cloud.

Manual Measurement of the Seedlings

The physical properties of the seedlings were manually measured to compare and validate the results from TLS scans. A flexible steel measuring tape was used to measure the maximum height, which was determined from the soil surface in the polybag to the tip of the seedlings. Then, the stem diameter of the seedlings was measured by using a stainless steel vernier calliper. Similar to the point clouds measurement, the stem diameter was measured at a height of 2 cm from the base or soil level (Figure 3). Both measurements, height and stem diameter, were repeated three times and averaged. In total, four temporal measurements were taken, and the interval between the measurements was two weeks.

Statistical Analysis

A t-test was used to check and observe the significant difference in mean height and mean stem diameter between the eight-month INF and NONF oil palm seedlings. In addition, a

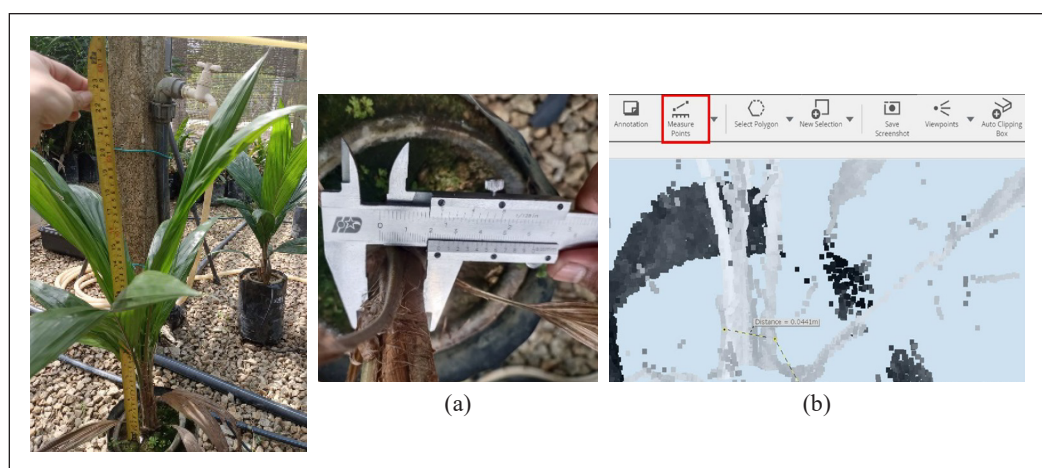


Figure 3. Measurements of oil palm seedlings: (a) manual; and (b) LiDAR point cloud measurements

Tukey HSD test was conducted to determine significant differences in the temporal changes between the measurements. Each statistical analysis was run using the JMP statistical software package (SAS Institute, Cary, USA). The α value was set to 0.05 confidence level. Furthermore, a correlation analysis was performed using Microsoft Excel (Microsoft, Redmond, WA) to observe the association between the manual measurement and TLS measurement. The closer the R^2 value to 1.0, the higher the correlation of the measurements. Figure 4 shows the steps of the method used in this study.

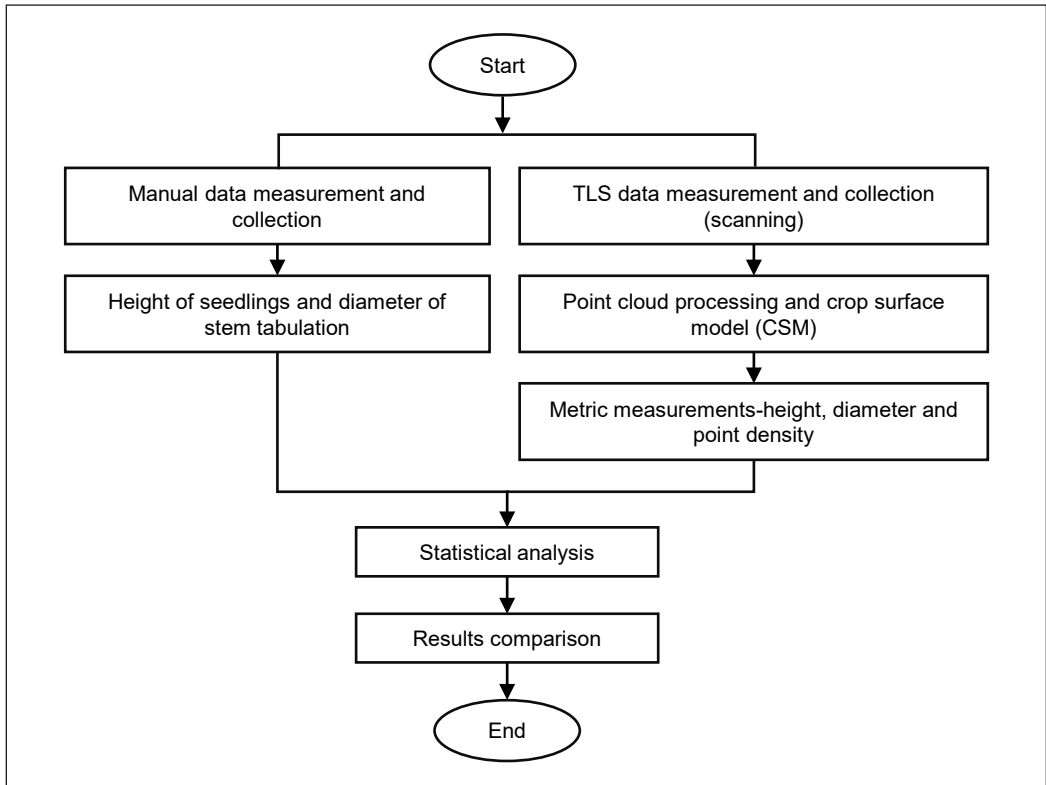


Figure 4. Flowchart of the method

RESULTS AND DISCUSSION

Analysis of Height and Stem Diameter

Figure 5 shows that the mean height of NONF and INF seedlings showed a continuous increment from the first measurement to the fourth measurement with R^2 values, 0.97 for the NONF seedlings and 0.98 for the INF seedlings. The mean height of the NONF seedlings increased with an average difference of $0.154 \text{ m} \pm 0.05 \text{ cm}$, while the mean height of the INF seedlings increased with an average difference of $0.139 \text{ m} \pm 0.05 \text{ cm}$ over the six weeks of TLS measurements in the nursery. Tukey HSD test showed significant differences between

all measurement times except the first and second measurements of the NONF seedlings (Table 1). The NONF seedlings had the highest and the lowest difference, which was from the second to the third measurement ($0.22 \text{ m} \pm 0.05 \text{ cm}$) and from the first to the second measurement ($0.073 \text{ m} \pm 0.05 \text{ cm}$), respectively. In all measurements, the mean height of NONF seedlings was significantly higher compared to INF seedlings at a 0.05 confidence level with all p-values less than 0.0001. The results show that the growth of NONF seedlings was better than the INF seedlings. NONF seedlings have a well-developed root system that can efficiently absorb water and nutrients from the soil. These nutrients are essential

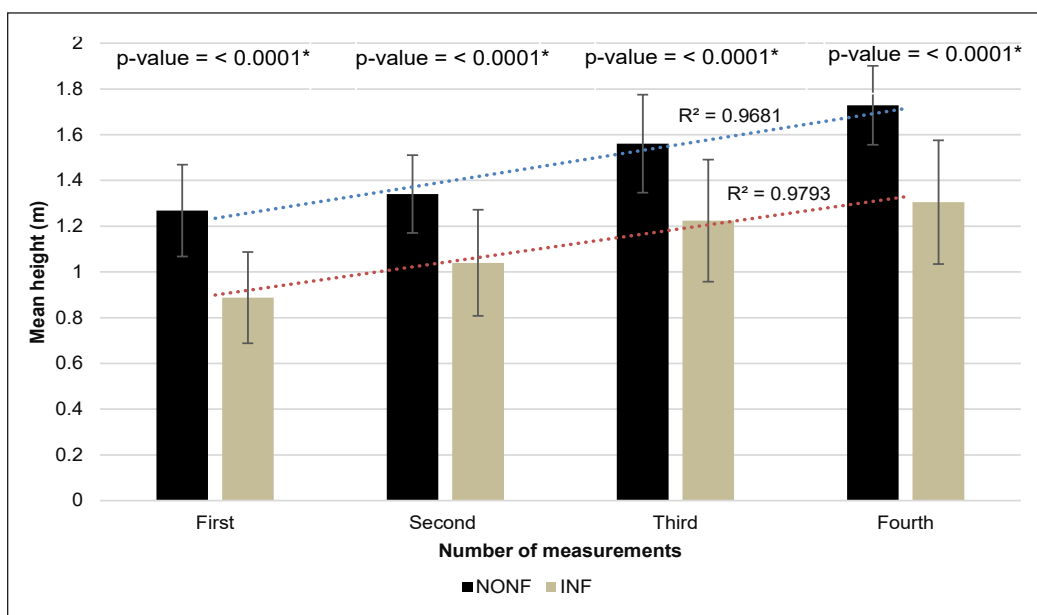


Figure 5. Mean height (\pm standard deviation) of the NONF and INF seedlings
 Note. * significant at 5% level

Table 1
 Tukey HSD test of temporal measurements for mean height and mean stem diameter

Type of Seedlings	Comparison of Measurements	Mean height		Mean stem diameter	
		Difference ($\text{m} \pm 0.05\text{cm}$)	p-value	Difference ($\text{mm} \pm 0.01 \text{ mm}$)	p-value
NONF	First and second	0.073	0.6126	2.487	0.2914
	Second and third	0.220	0.0026*	2.487	0.0835
	Third and fourth	0.168	0.0334*	4.092	0.5893
INF	First and second	0.152	0.0011*	0.018	1.000
	Second and third	0.184	<0.0001*	5.314	<0.0001*
	Third and fourth	0.081	0.0303*	6.887	<0.0001*

Note. * significant at 5% level

for growth, photosynthesis, and plant vigour. Meanwhile, the fungus *G.boninense* causes root rot (Figure 6), severely impairing the seedling's ability to absorb water and nutrients. This leads to nutrient deficiencies, which stunts growth and weakens the seedlings (Surendran et al., 2017). This means that BSR disease significantly affects the growth of oil palm seedlings. The results from Table 1 show that the height parameter is a better indicator for the temporal measurements, where all seedlings showed significant differences between the measurements except for the first and second measurements in NONF seedlings.

The mean stem diameter of NONF seedlings in Figure 7 showed an increasing trend from the first measurement to the fourth measurement with R^2 values of 0.69. The growth of the mean stem diameter of the NONF seedlings continuously increased with an average difference of $2.375 \text{ m} \pm 0.01 \text{ mm}$. In contrast, the INF seedlings showed a relatively slower growth rate with a mean diameter difference of $4.073 \text{ m} \pm 0.01 \text{ mm}$ over the six weeks of TLS measurements in the nursery. Even though the increase in stem diameter from the first to the second measurement and from the second to the third measurement were not significant, the trend showed an increase in healthy growth seedlings (Table 1). There was a slight decrease in the mean stem diameter from the third to the fourth measurement ($1.517 \pm 0.01 \text{ mm}$). The reduction in the mean diameter of the NONF seedlings between the third measurement and the fourth measurement might be due to the growth phase transition, where the seedlings might have transitioned from a rapid growth phase to a maintenance or stress response phase, where energy and resources were redirected to support other parts of the plant or to cope with environmental challenges, leading to temporary reductions in stem diameter (Huijser & Schmid, 2011). Meanwhile, the mean stem diameter of the INF seedlings was inconsistent with an R^2 value of 0.0005. It decreased from the first measurement to the second measurement ($0.018 \pm 0.01 \text{ mm}$), then increased at the third measurement ($5.314 \pm 0.01 \text{ mm}$) before drastically decreasing for the fourth measurement ($6.887 \pm 0.01 \text{ mm}$). The inconsistency of stem diameter might be due to the plant stress responses, where the response of the seedlings to *G.boninense* infection can fluctuate, with periods of higher stress leading to reduced growth and periods of recovery or compensatory growth (Shoresh et al., 2010). This could cause the stem diameter to increase at one point (as seen in the third measurement) and then decrease again as the infection progresses or as the seedlings exhaust their resources. In addition, the activation of defence mechanisms such as lignification (thickening of cell walls) or the



Figure 6. Root and stem bole damage to oil palm seedlings due to BSR

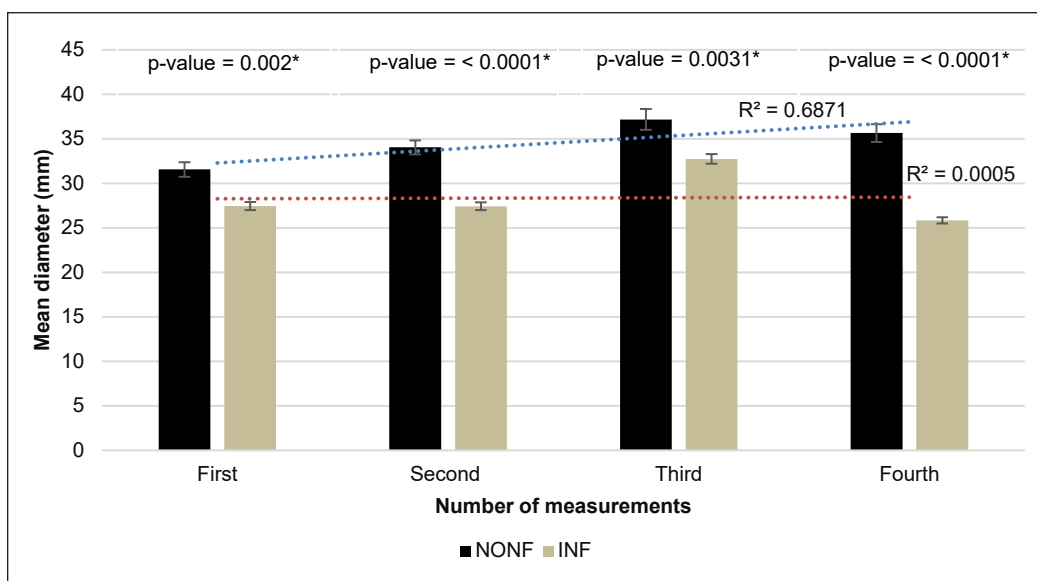


Figure 7. Mean diameter (\pm standard deviation) of the NONF and INF seedlings
 Note. * significant at 5% level

production of antifungal compounds by INF seedlings might temporarily affect growth rates, leading to inconsistent stem diameters (Faizah et al., 2022). The mean stem diameter of NONF seedlings was significantly larger than INF seedlings in all measurements at 0.05 confidence level with a p-value for the first measurement of 0.002, the second and fourth measurements were less than 0.0001, and the third measurement was 0.0031.

Analysis of Point Density

Figure 8 shows the average point density of the NONF and INF oil palm seedlings. The point density can be considered as the volume or surface area representation of the seedlings (Hosoi & Omasa, 2009). The first measurement of the point cloud was excluded due to an error in the NONF seedlings. The NONF seedlings presented higher point density from the second measurement to the fourth measurement compared to INF seedlings. It shows that NONF seedlings had normal and healthier growth compared to the stunted growth of INF seedlings. The point density for the NONF seedlings decreases from the second to the fourth measurement, with an average difference of point density of about 51 million points. Meanwhile, the point density of the INF seedlings increases from the second to third measurement and then decreases from the third to fourth measurement. The average difference in point density from the second to fourth measurement was about 23 million points. Growing plants often develop more complex surface structures with varied textures and angles. This increased roughness can scatter the LiDAR pulses more diffusely, reducing the number of pulses that return directly to the sensor and decreasing the point density

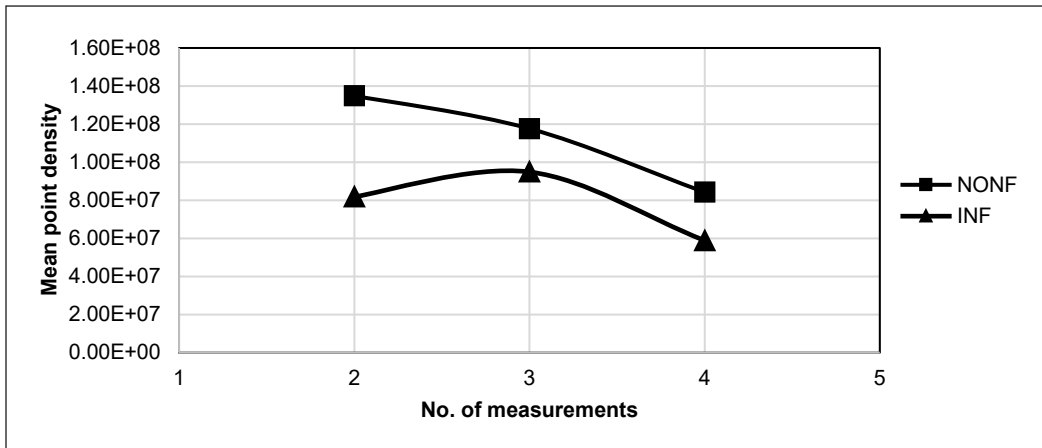


Figure 8. Point density of NONF seedlings and INF seedlings

(Rosette et al., 2012). Meanwhile, as the plant grows and the leaf orientation becomes more varied, some leaves may become angled in such a way that they reflect less laser energy back to the sensor, reducing point density (Gregorio & Llorens, 2021).

The differences in results between the NONF and INF seedlings were not likely because of fertiliser due to the same amount of fertiliser used for both types of seedlings. Two examples of infection modes are roots that came into contact with nearby infected palms and airborne basidiospores. The basidiospores of *G.boninense* initiate root damage by germinating on the part of oil palm seedlings and invading root tissues with hyphae and secreting enzymes that degrade the root structure (Bharudin et al., 2022). It was noted that contaminated soil tissues rather than airborne spores were the cause of the disease spreading to healthy roots so widely (Sanderson, 2005). The NONF seedlings maintained optimal chlorophyll content, which allowed for efficient photosynthesis, which was needed for growth and development. However, the INF seedlings showed chlorosis, which diminishes the plant's ability to perform photosynthesis and leads to less energy for growth. It was also stated that the effects of the BSR disease infection could be seen on the seedlings at four and seven months after planting, which affected the development and growth of the oil palm seedlings (Faizah et al., 2022). In addition, using eye and manual inspection, the colour and condition of the leaves in some INF seedlings turned from green to yellow and then necrotic and wilted. Also, fungal whitish fruiting bodies like the mushroom structure were seen around the base of the stem or in the soil near the roots.

Correlation Analysis

The correlation analysis for the TLS and manual methods showed a strong relationship in every measurement, with an average of R^2 equal to 0.95 for the height (Figure 9) and an average of R^2 equal to 0.93 for the stem diameter (Figure 10). The range value of R^2

from the first until the fourth readings of the height was between 0.9272 and 0.9646, while the stem diameter was between 0.8601 and 0.9810. The highest correlation was at the second measurement of stem diameter with R^2 equal to 0.981, and the lowest correlation was at the third measurement of stem diameter with R^2 equal to 0.8601. LiDAR technology is known for its high accuracy and precision in measuring dimensions. This accuracy translates into measurements that have a very high correlation with the manual method. Unlike manual measurements, which can vary depending on the person performing the measurement, LiDAR provides consistent results. The high correlation values showed that ground-based LiDAR, like TLS, was a reliable tool to measure the diameter and height of the seedlings. It was stated by Johnson and Liscio (2015) that the height determination of an object by using TLS was duplicable and accurate on a static object. Moreover, Maas et al. (2008) found that TLS was able to present good and accurate stem geometry data and was efficient for plants. Lumme et al. (2008) also mentioned that TLS was useful equipment for growth height estimation and could be used as a precision farming tool in agriculture. Instead of collecting data manually, TLS may be used for metric measurements since correlation analysis showed satisfactory outcomes. However, based on this study, more scan points are needed to obtain a clearer image of

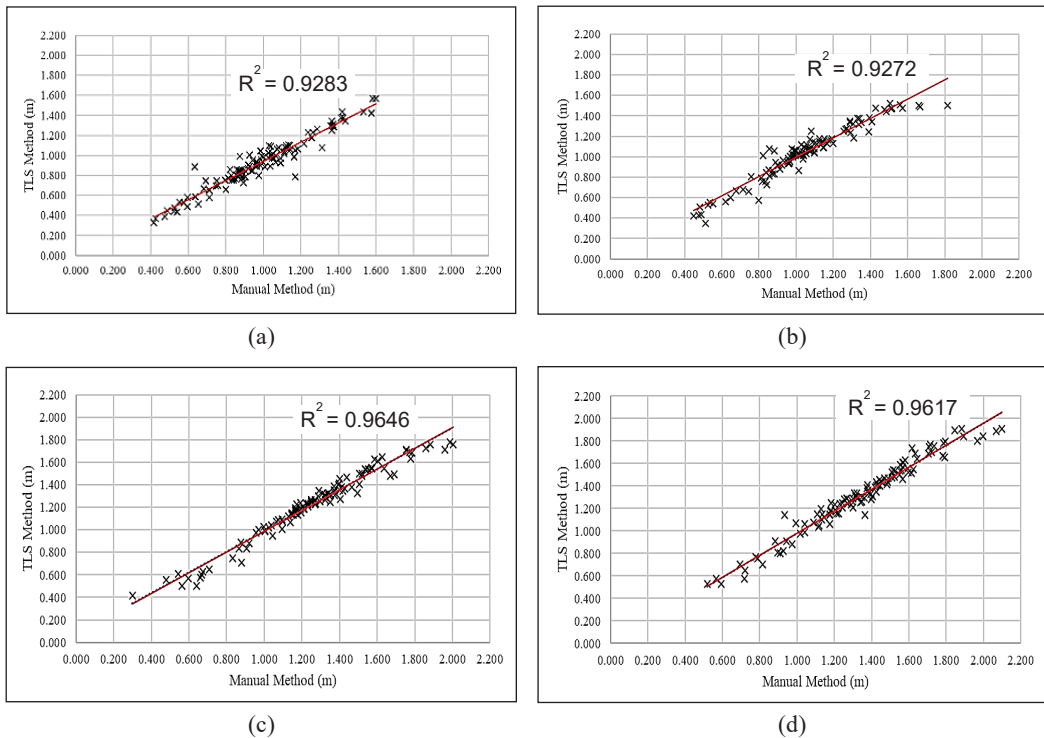


Figure 9. Correlation analysis of height: (a) First measurement; (b) Second measurement; (c) Third measurement; and (d) Fourth measurement

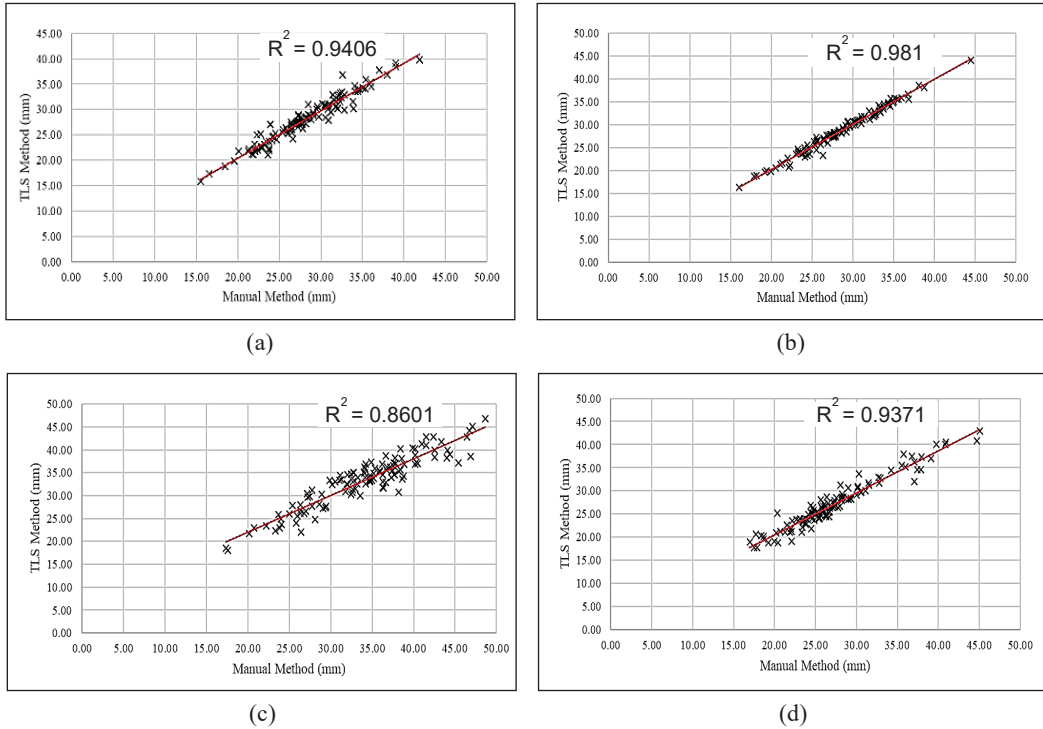


Figure 10. Correlation analysis of stem diameter: (a) First measurement; (b) Second measurement; (c) Third measurement; and (d) Fourth measurement

the stem cross-section. Overall, the high correlations (R^2 values) suggest that LiDAR is a reliable method that can produce results closely matching those obtained through manual measurements. The factors mentioned contribute to the strong relationship observed between the two measurement methods.

The metric features developed utilising point cloud data for BSR disease detection were height, stem diameter, and point density. The parameters or metric features could be utilised to distinguish between oil palm seedlings that are not infected with BSR and seedlings that are BSR-infected. This was the first in-depth analysis of oil palm seedlings in the nursery employing TLS to distinguish the changes brought by BSR disease. For the early diagnosis, management, and control of the disease, this cutting-edge image processing method using the physical characteristics of the oil palm seedlings was crucial. With the aid of pre-and post-processing facilities, it was also practical for in-situ applications. To achieve precision agricultural objectives, TLS offers information at the plant level. A sensing system utilising innovative algorithms and on-site technology may be able to deliver more accurate data to create a current health database for oil palm seedlings in nurseries.

Further research into the features of the oil palm seedlings could be undertaken for semi-auto calculation. Three characteristics - height, stem diameter, and point density

- could serve as the basis of the application. In this study, LiDAR showed a significant potential for BSR detection in oil palm seedlings, with accuracies of around 90%. Future health monitoring with LiDAR holds great promise, especially when coupled with chlorophyll data. For the classification of BSR diseases, further research may be done to establish a standard range based on the height, diameter, and point density of NONF and INF seedlings. Further research towards a model for BSR detection that includes height, diameter, and point density is possible. It has the potential to build complex models that take into consideration the leaf orientation, laser returns, and percentage of occlusion in oil palm seedlings.

The high-density LiDAR data is a useful tool for foliar and metric measurements. Although much effort needs to be made before realising this, these and other preliminary data may imply it. A 3D view of the seedlings could be used, and the view can be rotated to check the overlapping fronds between the seedlings. Additionally, by physically weighing the seedlings, the point density of the oil palm seedlings may be compared with their biomass. The outcomes further demonstrated the accuracy and dependability of TLS measurements. Despite its promise, the biggest disadvantage of the suggested method was the procedure of extracting the data, as some parameters required to be calculated manually. In the future, a deep learning technique might be used to automate the feature extraction process. The plantation manager could examine the condition of the seedlings in real time and create an alert system utilising an online platform. More research should be done to analyse oil palm seedlings with various levels of infection severity. Future research should give greater thought to adapting the data for a general approach to detecting *Ganoderma* disease because there are many potential methods to improve the procedures for usefulness and operation in plantation nurseries. To distinguish between oil palm seedlings that are not infected by BSR and BSR-infected seedlings, this study gives fundamental findings about the usage of static LiDAR.

The results of this work demonstrate the potential of TLS for precise 3D measurements of oil palm seedlings. It offers low-cost, high degree of information and is accurate, non-destructive, and high-precision measurements (Stovall et al., 2018). TLS allows for repeatable views and imaging from various angles and just comes at a one-time initial equipment cost. The benefits of the terrestrial laser scanner include its small size, portability, lightweight, and wide scanning range. For remote sensing, TLS sensors would be more economical and cost-effective. Both professionals and amateurs could easily manage it (Liang et al., 2016). This is the initial thorough investigation of the physical characteristics of oil palm seedlings utilising TLS for BSR disease. Additionally, it is a non-destructive measurement because it eliminates the need for human measurement, which might break and spoil the seedlings. Manual observation is time-consuming, individualised for each worker, and potentially exhausting. Continuous monitoring of each seedling is required

for naked-eye observation, which is time-consuming. Another concern is the lack of personnel in the plantation sector. The novel discovery of this study has the potential to close a knowledge gap in the field of laser scanning research and be an eye-opener for the community in this area.

TLS is regarded as an easy-to-use technology for information collection. Thus, since it is independent of the individual tasks of the workers, the process of scouting seedlings can be completed more quickly and effectively. Additionally, the use of a portable laser scanner may give greater flexibility and precision in terms of visuals and dimensions. Furthermore, LiDAR data may be crucial because it allows for the investigation and potential expansion of the model correlations between metric measurements and the level of BSR infection across a larger area. The progress and growth of laser scanning technology, which consistently enhances data quality, scanning speeds, and spatial coverage and offers a variety of platform types, bodes well for the proposed method in this study, even though it necessitates a processing procedure.

The initial setup costs for a ground-based laser scanner are around RM300,000, including the accessories, software and training for a single operator. Additional costs for calibration, software updates, and possible repairs are about RM 15,000. The advantages of ground-based LiDAR are less personnel needed; a single operator can handle the scanner with minimal assistance, saving labour costs and rapidly scanning large areas, reducing field time and field operation. The accuracy of the sensor is also extremely high, and the quality of the data is comprehensive, allowing for repeated analysis and additional measurements without returning to the field. Meanwhile, the manual vegetative measurements are around RM144,000 annually for four personnel. Manual measurements are arduous, and the fieldwork might take several hours to days, depending on the area size and the number of measurements. The data is usually recorded manually and entered in spreadsheets or databases, which can be time-consuming. The initial investment for a laser scanner is substantial, but the operational costs can be lower in the long run due to reduced labour and time efficiency and high-accuracy measurements.

Future research may examine the differences between BSR-infected oil palm seedlings and other symptoms of abiotic stresses such as drought. Fast and on-site diagnosis of plant diseases and long-term monitoring of plant health conditions are now possible, especially in situations with limited resources, thanks to portable imaging technologies (such as smartphones). By exchanging and transmitting data almost in real-time, the recent development of field-portable sensor equipment, such as smartphone devices or plant wearables, opens up promising new opportunities for the in-situ investigation of pathogens in the field (Li et al., 2020). Today's smartphones come with LiDAR sensors, making it possible to create mobile applications for identifying and categorising BSR illnesses using deep-learning object identification models.

CONCLUSION

In conclusion, the analysis demonstrates that the growth and development of oil palm seedlings are significantly impacted by Basal Stem Rot (BSR) disease, as evidenced by the differences in height, stem diameter, and point density between non-infected (NONF) and infected (INF) oil palm seedlings. The NONF seedlings consistently showed superior growth, indicating that healthy root systems are crucial for nutrient uptake and overall plant vigour. In contrast, the INF seedlings exhibited stunted growth due to the damaging effects of the *G. boninense* fungus, which impairs the roots' ability to absorb nutrients and water, leading to nutrient deficiencies and weakened seedlings. The use of ground-based LiDAR, specifically the Terrestrial Laser Scanner (TLS) technology, proved to be a reliable and precise method for monitoring the physical characteristics of oil palm seedlings. The high correlation between TLS and manual measurements highlights the potential of TLS as a non-destructive, accurate, and efficient tool for early detection and management of BSR disease in oil palm nurseries. Future research should focus on enhancing the TLS-based model by incorporating additional parameters like chlorophyll data and exploring the use of deep learning techniques for automated feature extraction. The findings from this study pave the way for more advanced and cost-effective approaches to disease management in agriculture, highlighting the value of integrating modern sensing technologies with traditional plantation practices.

ACKNOWLEDGEMENT

This research was funded by Universiti Putra Malaysia (UPM) under research project code GP-IPM/2021/9697200.

REFERENCES

- Akul, Y., Kumar, V., & Chong, K. P. (2018). Designing primers for loop-mediated isothermal amplification (LAMP) for detection of *Ganoderma boninense*. *Bulgarian Journal of Agricultural Science*, 24(5), 854-859.
- Azhar, T. M., Mustapha, J. C., Mazliham, S., & Boursier, P. (2011). Temporal analysis of basal stem rot disease in oil palm plantations: An analysis on peat soil. *International Journal of Engineering & Technology*, 11(3), 96-101.
- Azmi, A. N. N., Bejo, S. K., Jahari, M., Muharam, F. M., Yule, I., & Husin, N. A. (2020). Early detection of *Ganoderma boninense* in oil palm seedlings using support vector machines. *Remote Sensing*, 12(23), Article 3920. <https://doi.org/10.3390/rs12233920>
- Azmi, A. N. N., Khairunniza-Bejo, S., Jahari, M., Muharram, F. M., & Yule, I. (2021). Identification of a suitable machine learning model for detection of asymptomatic *Ganoderma boninense* infection in oil palm seedlings using hyperspectral data. *Applied Sciences*, 11(24), Article 11798. <https://doi.org/10.3390/app112411798>

- Azuan, N. H., Khairunniza-Bejo, S., Abdullah, A. F., Kassim, M. S. M., & Ahmad, D. (2019). Analysis of changes in oil palm canopy architecture from basal stem rot using terrestrial laser scanner. *Plant Disease*, *103*(12), 3218-3225. <https://doi.org/10.1094/PDIS-10-18-1721-RE>
- Bharudin, I., Wahab, A. F. F. A., Samad, M. A. A., Yie, N. X., Zairun, M. A., Bakar, F. D. A., & Murad, A. M. A. (2022). Review update on the life cycle, plant–microbe interaction, genomics, detection and control strategies of the oil palm pathogen *Ganoderma boninense*. *Biology*, *11*(2), Article 251. <https://doi.org/10.3390/biology11020251>
- Bornaz, L., & Rinaudo, F. (2004). Terrestrial laser scanner data processing. *XXth ISPRS Congress Istanbul*, *123*(123006), 1–4.
- Buja, I., Sabella, E., Monteduro, A. G., Chiriaco, M. S., De Bellis, L., Luvisi, A., & Maruccio, G. (2021). Advances in plant disease detection and monitoring: From traditional assays to in-field diagnostics. *Sensors*, *21*(6), Article 2129. <https://doi.org/10.3390/s21062129>
- Cabo, C., Ordóñez, C., López-Sánchez, C. A., & Armesto, J. (2018). Automatic dendrometry: Tree detection, tree height and diameter estimation using terrestrial laser scanning. *International Journal of Applied Earth Observation and Geoinformation*, *69*, 164-174.
- Fahey, T., Pham, H., Gardi, A., Sabatini, R., Stefanelli, D., Goodwin, I., & Lamb, D. W. (2020). Active and passive electro-optical sensors for health assessment in food crops. *Sensors*, *21*(1), Article 171. <https://doi.org/10.3390/s21010171>
- Faizah, R., Putranto, R. A., Raharti, V. R., Supena, N., Sukma, D., Budiani, A., Wening, S., & Sudarsono, S. (2022). Defense response changes in roots of oil palm (*Elaeis guineensis* Jacq.) seedlings after internal symptoms of *Ganoderma boninense* Pat. infection. *BMC Plant Biology*, *22*(1), Article 139. <https://doi.org/10.1186/s12870-022-03493-0>
- Farraji, H., Dahlan, I., & Eslamian, S. (2021). Water recycling from palm oil mill effluent. In S. Eslamian (Ed.), *Handbook of Water Harvesting and Conservation: Basic Concepts and Fundamentals* (pp. 307-320). John Wiley & Sons. <https://doi.org/10.1002/9781119478911.ch20>
- Girardeau-Montaut, D. (2016). *CloudCompare - Point Cloud Processing Workshop*. EDF R&D Telecom ParisTech. https://www.eurosd.net/sites/default/files/images/inline/04-cloudcompare_pcp_2019_public.pdf
- Gregorio, E., & Llorens, J. (2021). Sensing crop geometry and structure. In R. Kerry & A. Escolà (Eds.), *Sensing Approaches for Precision Agriculture* (pp. 59-92). Springer. https://doi.org/10.1007/978-3-030-78431-7_3
- Hillman, S., Wallace, L., Reinke, K., & Jones, S. (2021). A comparison between TLS and UAS LiDAR to represent eucalypt crown fuel characteristics. *ISPRS Journal of Photogrammetry and Remote Sensing*, *181*, 295-307. <https://doi.org/10.1016/j.isprsjprs.2021.09.008>
- Hilmi, N. H. Z., Idris, A. S., Maizatul-Suriza, M., Madihah, A. Z., & Nur-Rashyeda, R. (2022). Molecular PCR assays for detection of *Ganoderma* pathogenic to oil palm in Malaysia. *Malaysian Applied Biology*, *51*(1), 171-182. <https://doi.org/10.55230/mabjournal.v51i1.2201>
- Hosoi, F., & Omasa, K. (2009). Estimating vertical plant area density profile and growth parameters of a wheat canopy at different growth stages using three-dimensional portable lidar imaging.

- ISPRS Journal of Photogrammetry and Remote Sensing*, 64(2), 151-158. <https://doi.org/10.1016/j.isprsjprs.2008.09.003>
- Huijser, P., & Schmid, M. (2011). The control of developmental phase transitions in plants. *Development*, 138(19), 4117-4129. <https://doi.org/10.1242/dev.063511>
- Husin, N. A., Bejo, S. K., Abdullah, A. F., Kassim, M. S., & Ahmad, D. (2021). Relationship of oil palm crown features extracted using terrestrial laser scanning for basal stem rot disease classification. *Basrah Journal of Agricultural Sciences*, 34, 1-10. <https://doi.org/10.37077/25200860.2021.34.sp1.1>
- Husin, N. A., Khairunniza-Bejo, S., Abdullah, A. F., Kassim, M. S., Ahmad, D., & Aziz, M. H. (2020a). Classification of basal stem rot disease in oil palm plantations using terrestrial laser scanning data and machine learning. *Agronomy*, 10(11), Article 1624. <https://doi.org/10.3390/agronomy10111624>
- Husin, N. A., Khairunniza-Bejo, S., Abdullah, A. F., Kassim, M. S., Ahmad, D., & Azmi, A. N. (2020b). Application of ground-based LiDAR for analysing oil palm canopy properties on the occurrence of basal stem rot (BSR) disease. *Scientific Reports*, 10(1), Article 6464. <https://doi.org/s41598-020-62275-6>
- Husin, N. A., Khairunniza-Bejo, S., Abdullah, A. F., Kassim, M. S., & Ahmad, D. (2022). Multi-temporal analysis of terrestrial laser scanning data to detect basal stem rot in oil palm trees. *Precision Agriculture*, 23(1), 101-126. <https://doi.org/10.1007/s11119-021-09829-4>
- Husin, N. A., Khairunniza-Bejo, S., Abdullah, A. F., Kassim, M. S. M., & Ahmad, D. (2020c). Study of the oil palm crown characteristics associated with Basal Stem Rot (BSR) disease using stratification method of point cloud data. *Computers and Electronics in Agriculture*, 178, Article 105810. <https://doi.org/10.1016/j.compag.2020.105810>
- Johnson, M., & Liscio, E. (2015). Suspect height estimation using the Faro Focus3D laser scanner. *Journal of Forensic Sciences*, 60(6), 1582-1588. <https://doi.org/10.1111/1556-4029.12829>
- Khairunniza-Bejo, S., Shahibullah, M. S., Azmi, A. N. N., & Jahari, M. (2021). Non-destructive detection of asymptomatic *Ganoderma boninense* infection of oil palm seedlings using NIR-hyperspectral data and support vector machine. *Applied Sciences*, 11(22), Article 10878. <https://doi.org/10.3390/app112210878>
- Li, Z., Yu, T., Paul, R., Fan, J., Yang, Y., & Wei, Q. (2020). Agricultural nanodiagnosics for plant diseases: Recent advances and challenges. *Nanoscale Advances*, 2(8), 3083-3094. <https://doi.org/10.1039/C9NA00724E>
- Liang, X., Kankare, V., Hyypä, J., Wang, Y., Kukko, A., Haggrén, H., Yu, X., Kaartinen, H., Jaakkola, A., Guan, F., Holopainen, M., & Vastaranta, M. (2016). Terrestrial laser scanning in forest inventories. *ISPRS Journal of Photogrammetry and Remote Sensing*, 115, 63-77. <https://doi.org/10.1016/j.isprsjprs.2016.01.006>
- Liu, G., Wang, J., Dong, P., Chen, Y., & Liu, Z. (2018). Estimating individual tree height and diameter at breast height (DBH) from terrestrial laser scanning (TLS) data at plot level. *Forests*, 9(7), Article 398. <https://doi.org/10.3390/f9070398>
- Lumme, J., Karjalainen, M., Kaartinen, H., Kukko, A., Hyypä, J., Hyypä, H., Jaakkola, A., & Kleemola, J. (2008). Terrestrial laser scanning of agricultural crops. *The International Archives of the Photogrammetry, Remote Sensing and Spatial Information Sciences*, 37, 563-566.

- Maas, H. G., Bienert, A., Scheller, S., & Keane, E. (2008). Automatic forest inventory parameter determination from terrestrial laser scanner data. *International Journal of Remote Sensing*, 29(5), 1579-1593. <https://doi.org/10.1080/01431160701736406>
- Madihah, A. Z., Idris, A. S., & Rafidah, A. R. (2014). Polyclonal antibodies of *Ganoderma boninense* isolated from Malaysian oil palm for detection of basal stem rot disease. *African Journal of Biotechnology*, 13(34), 3455-3463. <https://doi.org/10.5897/AJB2013.13604>
- Madihah, A. Z., Maizatul-Suriza, M., Idris, A. S., Bakar, M. F. A., Kamaruddin, S., Bharudin, I., Bakar, F. D. A., & Murad, A. M. A. (2018). Comparison of DNA extraction and detection of *Ganoderma*, causal of basal stem rot disease in oil palm using loop-mediated isothermal amplification. *Malaysian Applied Biology*, 47(5), 119-127.
- Naidu, Y., Siddiqui, Y., Rafii, M. Y., Saud, H. M., & Idris, A. S. (2018). Inoculation of oil palm seedlings in Malaysia with white-rot hymenomycetes: Assessment of pathogenicity and vegetative growth. *Crop Protection*, 110, 146-154. <https://doi.org/10.1016/j.cropro.2018.02.018>
- Parveez, G. K. A., Kamil, N. N., Zawawi, N. Z., Ong-Abdullah, M., Rasuddin, R., Loh, S. K., Selvaduray, K. R., Hoong, S. S., & Idris, Z. (2022). Oil palm economic performance in Malaysia and R&D progress in 2021. *Journal of Oil Palm Research*, 34(2), 185-218. <https://doi.org/10.21894/jopr.2022.0036>
- Pitkänen, T. P., Raunonen, P., Liang, X., Lehtomäki, M., & Kangas, A. (2021). Improving TLS-based stem volume estimates by field measurements. *Computers and Electronics in Agriculture*, 180, Article 105882. <https://doi.org/10.1016/j.compag.2020.105882>
- Rees, R. W., Flood, J., Hasan, Y., Potter, U., & Cooper, R. M. (2009). Basal stem rot of oil palm (*Elaeis guineensis*); Mode of root infection and lower stem invasion by *Ganoderma boninense*. *Plant Pathology*, 58(5), 982-989. <https://doi.org/10.1111/j.1365-3059.2009.02100.x>
- Rosette, J., Suárez, J., Nelson, R., Los, S., Cook, B., & North, P. (2012). Lidar remote sensing for biomass assessment. *Remote Sensing of Biomass—Principles and Applications*, 24, 3-27. <https://doi.org/10.5772/17479>
- Sanderson, F. R. (2005). An insight into spore dispersal of *Ganoderma boninense* on oil palm. *Mycopathologia*, 159(1), 139-141. <https://doi.org/10.1007/s11046-004-4436-2>
- Santoso, H., Gunawan, T., Jatmiko, R. H., Darmosarkoro, W., & Minasny, B. (2011). Mapping and identifying basal stem rot disease in oil palms in North Sumatra with QuickBird imagery. *Precision Agriculture*, 12(2), 233-248. <https://doi.org/10.1007/s11119-010-9172-7>
- Shoresh, M., Harman, G. E., & Mastouri, F. (2010). Induced systemic resistance and plant responses to fungal biocontrol agents. *Annual Review of Phytopathology*, 48(1), 21-43. <https://doi.org/10.1146/annurev-phyto-073009-114450>
- Stovall, A. E., Anderson-Teixeira, K. J., & Shugart, H. H. (2018). Assessing terrestrial laser scanning for developing non-destructive biomass allometry. *Forest Ecology and Management*, 427, 217-229. <https://doi.org/10.1016/j.foreco.2018.06.004>
- Surendran, A., Siddiqui, Y., Saud, H. M., & Manickam, N. S. A. S. (2017). The antagonistic effect of phenolic compounds on ligninolytic and cellulolytic enzymes of *Ganoderma boninense*, causing basal stem rot

in oil palm. *International Journal of Agriculture & Biology*, 19, 1437-1446. <https://doi.org/10.17957/IJAB/15.0439>

Wagers, S., Castilla, G., Filiatrault, M., & Sanchez-Azofeifa, G. A. (2021). Using TLS-measured tree attributes to estimate aboveground biomass in small black spruce trees. *Forests*, 12(11), Article 1521. <https://doi.org/10.3390/f12111521>

Yap, P., Rosdin, R., Abdul-Rahman, A. A. A., Omar, A. T., Mohamed, M. N., & Rahami, M. S. (2021). Malaysian sustainable palm oil (MSPO) certification progress for independent smallholders in Malaysia. In *IOP Conference Series: Earth and Environmental Science* (Vol. 736, No. 1, p. 012071). IOP Publishing. <https://doi.org/10.1088/1755-1315/736/1/012071>

Zevgolis, Y. G., Alsamail, M. Z., Akriotis, T., Dimitrakopoulos, P. G., & Troumbis, A. Y. (2022). Detecting, quantifying, and mapping urban trees' structural defects using infrared thermography: Implications for tree risk assessment and management. *Urban Forestry & Urban Greening*, 75, Article 127691. <https://doi.org/10.1016/j.ufug.2022.127691>